Available online at www.sciencedirect.com
SCIENCE DIRECT®
Journal of Membrane Science 249 (2005) 163–172
journal of MEMBRANE SCIENCE
www.elsevier.com/locate/memsci

Membrane formation by dry-cast process Model validation through morphological studies

Sacide Alsoy Altinkaya[a,*], Hacer Yenal[a], Bulent Ozbas[b]

[a] *Department of Chemical Engineering, Izmir Institute of Technology, Gulbahce Koyu, Urla-Izmir 35437, Turkey*
[b] *Department of Materials Science and Engineering, Izmir Institute of Technology, Gulbahce Koyu, Urla-Izmir 35437, Turkey*

Received 26 February 2004; received in revised form 2 September 2004; accepted 4 October 2004
Available online 23 December 2004

Abstract

Asymmetric membranes were prepared by dry-cast phase inversion technique from a cellulose acetate, acetone, water solution in order to assess the validity of the mathematical model recently developed by us. Based on the model predictions, general structural characteristics of the membranes were determined by plotting the composition paths on the ternary phase diagram and polymer concentration profile at the first moment of precipitation. Composition paths on the ternary phase diagram enable the assessment of whether a phase separation occurs and allow prediction of inception time and duration of the phase separation. The polymer distribution at the moment of precipitation provides a rough thickness of the high polymer concentration region near the interface and a pore distribution of the sublayer structure. The effects of polymer/nonsolvent ratio in the casting solution, the initial film thickness, evaporation temperature, relative humidity and velocity of air were investigated. Model predictions were compared with the morphological analysis conducted using scanning electron microscopy. Results show that diffusion formulation plays an important role in capturing the accurate structure of the membrane from the model predictions.

Keywords: Asymmetric membrane; Dry-cast process; Morphological studies; Cellulose acetate; Phase diagram

1. Introduction

Polymeric membranes are usually produced by phase inversion techniques. In these techniques, an initially homogeneous polymer solution becomes thermodynamically unstable due to different external effects and phase separates into polymer-lean and polymer-rich phases. The polymer-rich phase forms the matrix of the membrane, while the polymer-lean phase, rich in solvents and nonsolvents, fills the pores. Depending on the evaporation/quenching conditions, initial thickness and composition of the polymer solution, various membrane structures ranging from dense to highly asymmetric can be obtained. The asymmetric membranes are characterized by a very thin, but relatively dense skin layer supported by a more open porous sublayer. The fraction of the dense skin layer determines the separation performance while the porous sublayer provides mechanical support and influences the overall flow resistance.

The manufacture of polymeric membranes by phase inversion techniques is not rigorous. However, slight change in the membrane fabrication process can significantly affect the ultimate membrane morphology as well as membrane performance. Thus, there has been considerable motivation for developing mathematical models for phase inversion techniques to eliminate extensive trial and error experimentation and optimize membrane preparation conditions. Most of these mathematical models and corresponding experimental work is focused on wet cast [1–13] and thermal cast processes [10,14–16]. However, there are relatively few quantitative studies on the dry-cast process even though this technique offers some advantages compared to other phase inversion techniques. The first unsteady-state, one dimensional model for a dry-casting process of a ternary mixture was developed

* Corresponding author. Tel.: +90 232 750 6273; fax: +90 232 750 6196.
E-mail address: sacidealsoy@iyte.edu.tr (S.A. Altinkaya).

0376-7388/$ – see front matter © 2004 Elsevier B.V. All rights reserved.
doi:10.1016/j.memsci.2004.10.008

by Shojaie et al. [17] which allows for local film shrinkage due to excess volume of mixing effects as well as evaporative solvent and nonsolvent loss. In a following paper, they investigated the effects of initial composition and casting thickness on the membrane structure and validated the model using independent real-time measurements of the process variables [18]. In addition, morphological studies were utilized to further justify the model predictions. Matsuyama et al. [19] prepared various types of porous membranes by dry-cast process in several cellulose acetate/acetone/nonsolvent systems. The effects of the ratio of the weight fraction of nonsolvent to polymer, the thickness of the membrane, and the type of nonsolvent on the structure of membranes were investigated both theoretically and experimentally. Recently, Alsoy Altinkaya and Ozbas [20] have shown that appropriate formulation of the ternary diffusivities and accurate parameters used in these expressions form the basis of accurate membrane modeling. The majority of other previous experimental studies of dry-casting processes are concerned with the formation of macroviods [18,21–23] in which different hypotheses were proposed and various experimental techniques following the initiation and growth of the macrovoids were discussed.

In this study, the dry-cast model developed previously by our group [20] was further validated by comparing the model predictions with the morphological studies. Our model has some unique features and differs from Shojaie et al.'s model [17] in few ways. Specifically, Shojaie et al.'s model [17] (referred to here as the SS model) includes a one dimensional unsteady-state heat transfer equation, while, in our model temperature through the membrane forming solution and the substrate is uniform and the heat transfer is approximated by a lumped parameter approach. This approximation is fairly reasonable since resistance to heat transfer in the gas phase is much greater than in the polymer solution or the substrate layer. In addition, the validity of this assumption was confirmed by the predictions of Shojaie et al. [17] which indicate flat temperature profiles at different times during membrane formation. The SS model incorporates effects of volume change on mixing. In our model, it is assumed that the partial specific volume of the components are independent of the composition. This assumption is made based on the predictions of Alsoy and Duda [24]. Their study indicates that for most polymer–solvent systems, the influence of diffusion-induced convection associated with volume changes on mixing can be neglected in the analysis of sorption processes. The correction term for the volume change on mixing is usually small and negligible if the volume change on mixing is below 4%. Experimental studies indicate that most polymer–solvent systems do not show large deviations from ideal volumetric behaviour, and the absolute value is typically 1–2% or less [25–28]. With this assumption, presenting the problem in terms of volume average velocity reduces the complexity and the number of governing equations. As a consequence, the procedures utilized in our study greatly reduce the computer power required to describe complex membrane formation processes. In our study, the friction-based diffusion model proposed by Alsoy and Duda [29] is used to predict the multicomponent diffusivities. According to this model, multicomponent diffusivities are only a function of the self-diffusion coefficients and the thermodynamic factor of the corresponding component and they can be easily determined from readily accessible thermodynamic and self-diffusion data. The validity of this theory has previously been confirmed by: (a) predicting experimental values of the principal and cross coefficients for a ternary organic mixture [30]; (b) applying the diffusion model to predict the drying behaviour of different ternary systems [29,31]. Equations in the SS model involve friction coefficients that no experimental measurements are available on these coefficients or how they change as a function of composition [17]. It is important to recognize that our dry-cast model is a completely predictive one, in that it does not contain any adjustable parameters. The predictions are based only on conservation laws, solution thermodynamics, and measured and correlated values of relevant transport properties.

In the first part of the paper, the effects of initial composition and the thickness of the casting solution as well as the environmental conditions such as relative humidity, temperature and the velocity of air on the structure of the membrane are investigated. In the second part, the role of diffusion formalism in capturing the accurate structure of the membrane is clearly illustrated by comparing the morphological studies with the model predictions from three different alternative diffusion models.

2. Experimental

2.1. Materials

Membranes were prepared from ternary solutions consisting of cellulose acetate, acetone and water using a dry-casting method. Cellulose acetate (CA) with a molecular weight of 50,000 g/mol and an acetyl content of 39.7% was purchased from Aldrich. Acetone with a purity of 99% obtained from Merck was used as the solvent, and distilled and deionized water was used as the nonsolvent. The CA was dried in an oven above 100 °C for several hours prior to use. No further purification was applied to the materials.

2.2. Membrane preparation and characterization

The cellulose acetate solution was cast onto a 6 cm × 18 cm glass substrate with the aid of an automatic film applicator (Sheen Instruments Ltd., model number: 1133N). The initial thickness of the cast film was adjusted by a four-sided applicator with the gap sizes of 150, 200, 250 and 300 μm. Immediately after casting, the glass support was transferred into an environmental chamber (Angelantoni Industrie, Italy, Challenge Series, model number: CH250) and

kept there for 2 h to allow for evaporation of both the solvent and the nonsolvent. For experiments shown in this study, the temperature and the relative humidity of the air was adjusted within the range of 25 °C–50 °C and 25%–50%, respectively. After 2 h of air exposure within the environmental chamber, the cast films were allowed to dry further for a minimum of 24 h at room temperature prior to removal from the glass substrate.

Morphology of the membranes was examined by scanning electron microscopy (SEM) on a Philips XL-30SFG model. Samples were coated with gold palladium using a Magnetron Sputter Coating Instrument. The thickness of the dense skin layer, the overall porosity, and the average pore size were determined from image analysis of SEM micrographs showing cross sections of the membranes.

3. Determination of phase diagrams and composition paths

The polymeric membrane formation by the dry-casting method is a complicated process due to phase separation, and simultaneous heat and mass transfer mechanisms controlled by complex thermodynamic and transport properties of polymer solutions. Model equations consist of coupled unsteady-state heat and mass transfer equations, film shrinkage, and complex boundary conditions especially at the polymer–gas interface. The predictions from the model provide composition paths, temperature, and membrane thickness. The onset of phase separation is determined when the composition paths of the solution–air and solution–substrate interfaces touch the binodal curve. A robust algorithm was developed to construct the ternary phase diagrams using the Flory Huggins thermodynanic theory with constant interaction parameters. In previous studies, the concentration dependence of the water/cellulose acetate binary interaction parameter was ignored in order to avoid the use of any adjustable parameter [4,17]. Yilmaz and McHugh [32] have shown that shapes of the binodal and spinodal curves generated from constant and concentration dependent solvent–nonsolvent interaction parameters are similar. They concluded that ternary phase diagrams can be calculated using constant solvent/nonsolvent interaction parameters within the characteristic experimental range. Furthermore, Yilmaz and McHugh [32] point out the fact that data for the concentration dependence of solvent–polymer interaction parameters are quite limited and experimental difficulties limit their accuracy. Thus, empirical fits of low order (i.e., linear form) are used although they have relatively poor accuracy. Based on this limitation and their predictions, we have decided to use constant interaction parameters in our model. Highly nonlinear model equations were solved using finite difference approximations with a variable grid size. The details of the numerical solution procedure and the algorithm used in constructing the phase diagram can be found in the thesis of Ozbas [33].

4. Results and discussion

4.1. Effect of polymer (P)–nonsolvent (NS) ratio

The impact of altering the composition of the casting solution and the bath is well documented for wet phase inversion techniques [34–47]. However, there are relatively few quantitative studies on the morphology of the membranes prepared by dry-casting methods [18,19,22]. To investigate the effect of the casting composition on the final structure of the membrane, weight fraction of acetone (S) was kept constant at 80% while the ratio of weight percent of cellulose acetate (P) to water (NS) was varied at 5/15, 10/10 and 15/5. The ternary solutions were then allowed to evaporate within the environmental chamber at 25 °C and 50% relative humidity. In order to validate the dry-cast model developed previously by us, simulations were performed for these experimental conditions denoted by Cases R1, R2 and R3, in Table 1. Based on model predictions, information about the structure of the membrane was obtained by plotting the composition paths on the ternary phase diagram and the polymer distribution at the first moment of precipitation. For example, the concentration paths in time for the substrate/solution (glass facing side) and solution/air interface (air facing side) for Case R2 are shown in Fig. 1. According to this plot, phase separation takes place and the concentration paths of the two interfaces cross the binodal curve at markedly different times and different concentrations. Based on these two observations, one might expect that the casting conditions represented by Case R2 will produce porous asymmetric membranes in which the upper surface is more dense than the lower surface. The precipitation times calculated for each case are tabulated in Table 2. The results show the expected trend of decreasing precipitation time with decreasing P/NS ratio in the initial casting solution. In all cases, the concentration path of the solution/air interface crosses the binodal curve at earlier times

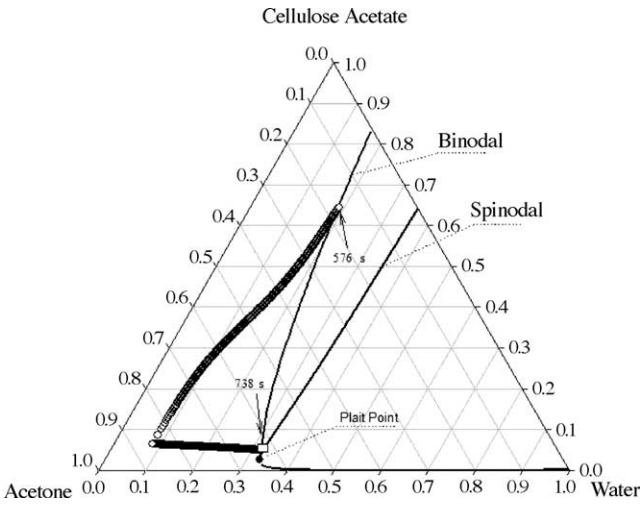

Fig. 1. Concentration paths of water, acetone and cellulose acetate for Case R2: (◯) solution/air interface; (□): solution/substrate interface.

Table 1
Experimental conditions

Cases	Weight fractions			Air temperature (°C)	Initial casting thickness (μm)	Relative humidity (%)	Overall porosity (%)	Average radius of the pores (μm)	Thickness of skin layer (%)
	CA	Acetone	Water						
R1	0.05	0.80	0.15	25	300	50	–	–	–
R2	0.10	0.80	0.10	25	300	50	35.9	1.5	3.7
R3	0.15	0.80	0.05	25	300	50	10.9	0.7	14.7
R4	0.10	0.80	0.10	25	200	50	35.9	1.3	5.9
R5	0.10	0.80	0.10	50	300	50	39.9	2.2	4.1
R6	0.10	0.80	0.10	25	300	25	33.9	1.6	4.2
R7	0.10	0.80	0.10	18	300	40	–	–	–

and the calculation was continued until the substrate interface has also precipitated. In other studies such as Shojaie et al.'s work [17,18], solid/liquid and liquid/gas interfaces reach the phase boundary at markedly different times. We are aware of the fact that our model, as well as most of the other mathematical models is based on purely homogeneous diffusion and they are no longer valid once binodal line is reached. However, they provide an insight about the initial dynamics of the process by quantifying the interactions among the material and process variables. Asymmetric membranes are usually characterized by the fraction of dense and porous layers, the shape and size of the pores, and the pore size distribution. Theoretically, the polymer distribution at the onset of precipitation provides a rough thickness of dense skin layer near the interface and the pore distribution of the sublayer structure. Examination of the polymer concentration profiles for Cases R1, R2 and R3 in Fig. 2 leads to the following conclusions regarding the effect of increased P/NS ratio in the casting solution. (a) Within the top 10% of the free surface, the change in polymer concentration is smallest (39%) when P/NS ratio is 15/5 and largest (45%) when this ratio is 5/15. In addition, the polymer volume fraction at the solution–air interface is largest for Case 3, being around 0.75. Thus, higher polymer concentrations in a large region of the membrane leads to formation of denser and thicker skins at the solution–air interface. (b) Low porosity, graded–pore sublayer structures are favored. Membrane prepared from a casting solution having P/NS ratio of 5/15 will have uniform porosity especially on the side facing the glass (substrate–solution interface) while the porosity of the membrane will change throughout the cross section as this ratio is increased to 15/5. It should be reiterated that polymer concentration profiles in Fig. 2 correspond to the first moment of precipitation, and after that time we did not utilize any simulation results in order to obtain any information about the final structure of the membrane.

Table 2
Precipitation times

Cases	Weight fractions			Substrate side (s)	Air side (s)
	CA	Acetone	Water		
R1	0.05	0.80	0.15	586	498
R2	0.10	0.80	0.10	738	576
R3	0.15	0.80	0.05	800	700
R4	0.10	0.80	0.10	439	381
R5	0.10	0.80	0.10	405	296
R6	0.10	0.80	0.10	877	640
R7	0.10	0.80	0.10	–	–

The scanning electron micrographs (SEM) of the cross sections of the membranes prepared from casting conditions corresponding to Cases R1, R2 and R3, respectively, are shown in Figs. 3–5. One can clearly see from these figures that with increased P/NS ratio in the casting solution, the membrane became much more dense and the thickness of the dense top layer increased. Fig. 3 indicates that membrane prepared from a P/NS ratio of 5/15 is highly porous and porosity is almost the same throughout the sublayer structure. These observations are in complete agreement with our model predictions as discussed above. The fraction of dense skin layer, the overall porosity and the average pore sizes of the membranes measured by the image analyzing software are given in Table 1. These values could not be determined for the membranes prepared from a casting solution with a P/NS ratio of 5/15 due to a highly porous structure of the membrane and connectivity of the pores. Morphological characterization results listed in Table 1 are qualitative rather than quantitative. However, with the aid of these results, certain trends in the morphologies obtained from different casting conditions become apparent.

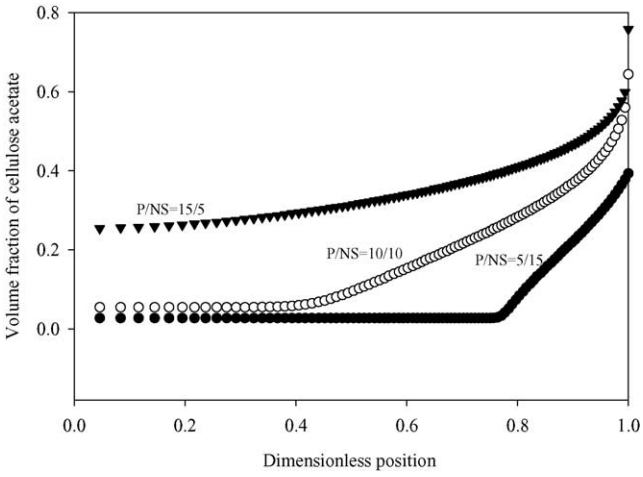

Fig. 2. Polymer concentration profiles in the membrane for Cases R1, R2 and R3 at the moment of precipitation.

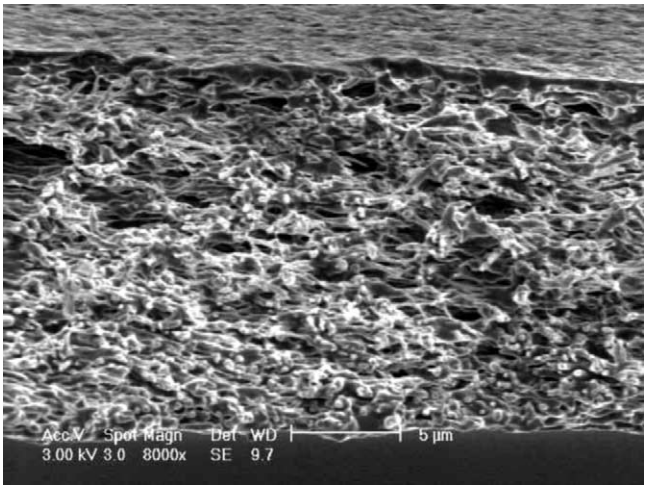

Fig. 3. Scanning electron micrograph of the membrane cast from a ternary water/cellulose acetate/acetone solution for the casting conditions corresponding to Case R1.

4.2. Effect of initial thickness of the casting solution

To investigate the effect of initial thickness of the casting solution on the final membrane structure, membranes were cast from a solution composed of 10% CA, 80% acetone and 10% water using a four-sided applicator with a gap size of 200 μm. For Case R4, the initial film thickness is 200 μm and all other experimental conditions are identical to those of Case R2. Comparison of the precipitation times for these two cases indicate that decreasing the initial film thickness leads to faster phase separation due to a decrease in resistance of the diffusion controlled mass transfer region. The polymer distributions for both cases shown in Fig. 6 indicate that decreasing the initial thickness of the casting solution leads to the formation of a thicker skin layer while the pore distribution and the porosity of both membranes remain similar. To determine

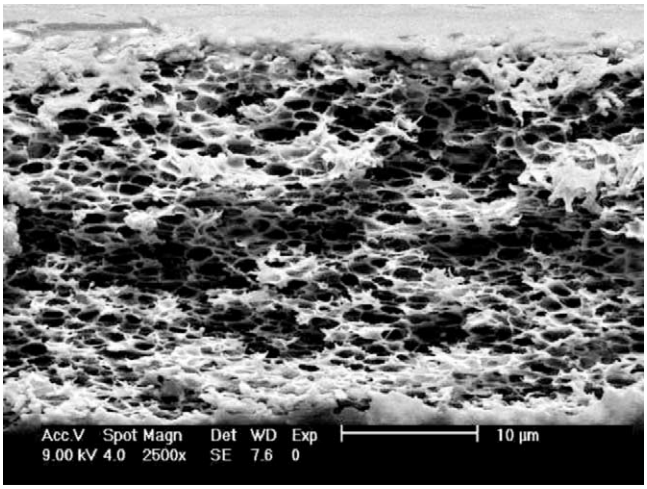

Fig. 4. Scanning electron micrograph of the membrane cast from a ternary water/cellulose acetate/acetone solution for the casting conditions corresponding to Case R2.

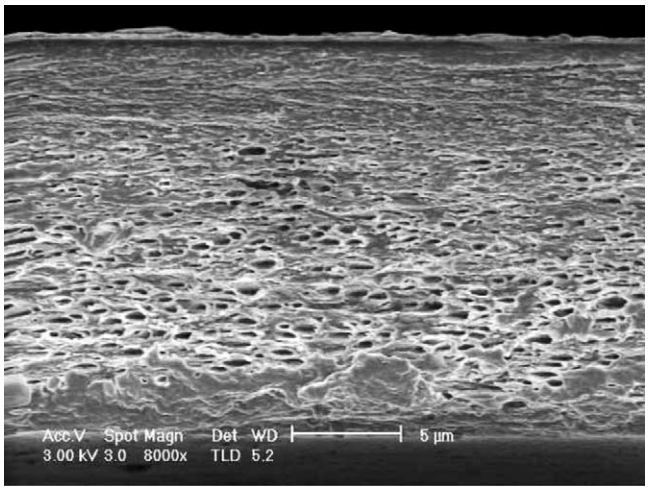

Fig. 5. Scanning electron micrograph of the membrane cast from a ternary water/cellulose acetate/acetone solution for the casting conditions corresponding to Case R3.

the fraction of dense skin layer from such a plot, we have defined the surface skin thickness as the distance between the free surface and the point at which the concentration of polymer decreases by 10%. According to this qualitative criteria, the percentage of dense skin layer was found to increase from 0.46% to 2.45% as the initial thickness of the casting solution was decreased from 300 μm to 200 μm. Furthermore, the results in Fig. 6 imply that decreasing the initial film thickness favors the formation of less asymmetric membrane structures since the difference in polymer concentrations at the top and bottom surfaces is smaller. These predictions were confirmed with SEM micrographs of two cases shown in Figs. 4 and 7. The analysis of the cross section of the membranes indicated that with decreasing initial film thickness, the overall porosity did not significantly change, the pore sizes slightly decreased, and the percentage of dense skin layer increased from 3.7% to 5.9%. Similar behavior was reported by Matsuyama et al. [19]. In particular, they found that with the decrease in the

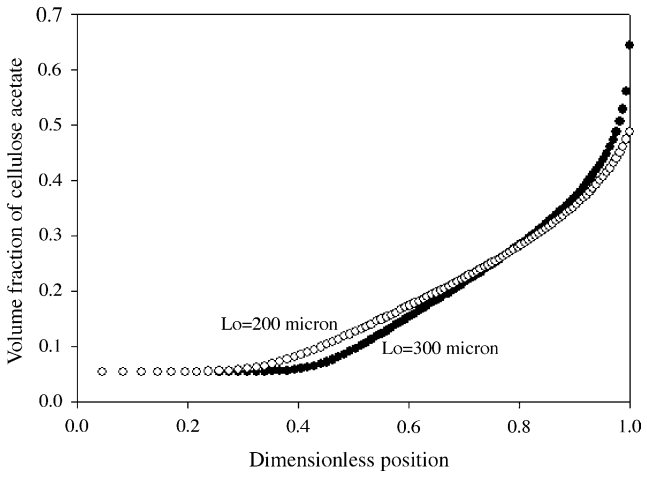

Fig. 6. Polymer concentration profiles in the membrane for Cases R2 and R4 at the moment of precipitation.

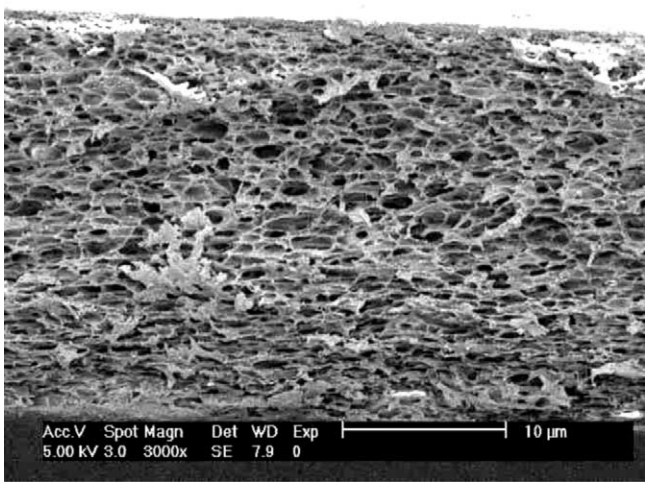

Fig. 7. Scanning electron micrograph of the membrane cast from a ternary water/cellulose acetate/acetone solution for the casting conditions corresponding to Case R4.

initial casting thickness, the asymmetric structures were suppressed and changed to much more dense skin structures.

4.3. Effect of evaporation temperature

The effect of evaporation temperature on the final structure of the membrane was investigated by increasing the temperature within the environmental chamber from 25 °C to 50 °C. All other experimental conditions for Case R5 are identical to those of Case R2. Comparison of the precipitation times tabulated in Table 2 indicate the expected trend of decreasing precipitation time with increased evaporation temperature due to faster diffusion of both acetone and water in the solution as well as faster evaporation of both components from the surface. Polymer distributions in each case plotted in Fig. 8 indicate that increasing air temperature will cause formation of more dense structures near the top surface. According to the qualitative criteria we have defined, percent of skin layer

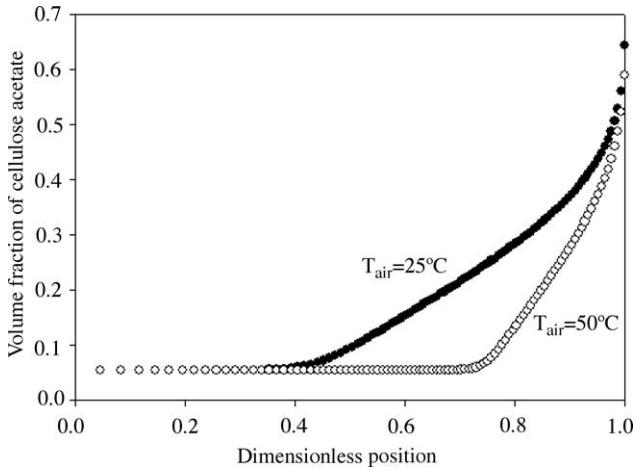

Fig. 8. Polymer concentration profiles in the membrane for Cases R2 and R5 at the moment of precipitation.

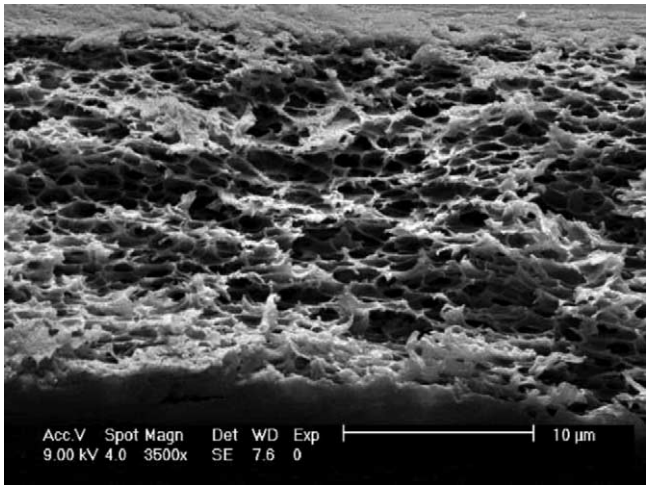

Fig. 9. Scanning electron micrograph of the membrane cast from a ternary water/cellulose acetate/acetone solution for the casting conditions corresponding to Case R5.

increases from 0.46% to 0.54% as the evaporation temperature is increased from 25 °C to 50 °C. In addition, results in Fig. 8 show that higher evaporation temperature will favor less asymmetric and more porous sublayer structures except in a small region facing the glass side. The corresponding scanning electron micrograph of the final film morphology prepared at the evaporation temperature of 50 °C is shown in Fig. 9. The analysis of the cross section in this figure revealed that, with increased evaporation temperature, the total thickness of the membrane decreased while both overall porosity and the percent of dense skin layer increased as predicted by the model. In addition, the pore sizes also increased. Similar trends were observed by other investigators. Young et al. [48] have found that the rise in the evaporation temperature during the dry-cast process changed the membrane structure of crystalline poly(ethylene-co-vinyl alcohol) (EVAL) from a particulate to a dense morphology. The results reported by Mohamed and Al-Dossary [47] have indicated that the use of higher evaporation temperatures during the membrane formation resulted in lower water permeabilities due to a thicker dense skin layer formed at the membrane surface.

4.4. Effect of relative humidity

To investigate the effect of relative humidity on the structure of the membrane, the dry-cast experiment was conducted at conditions corresponding to Case R6 in Table 1. Comparison of the precipitation time for Case R6 with that of Case R2 indicate that with increasing relative humidity of air, the solution/air and substrate/solution interfaces enter into the phase diagram more rapidly, but not at the same time. This is due to a decrease in driving force for the evaporation of water, thus trapping more residual water in the solution. Consequently, more rapid phase separation takes place. This prediction is consistent with the observation of Park et al. [49]. The predictions of the polymer distribution profiles shown in Fig. 10

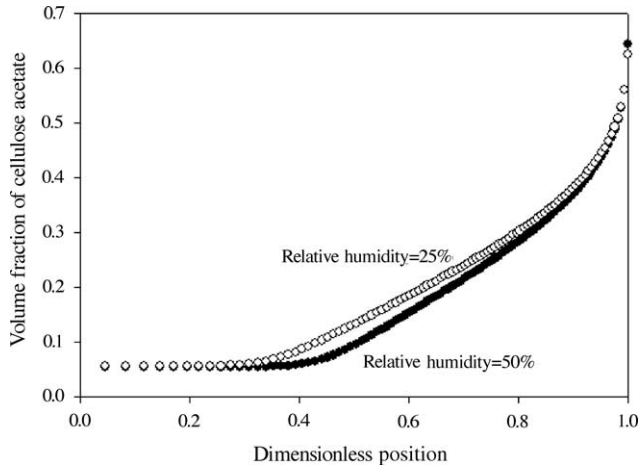

Fig. 10. Polymer concentration profiles in the membrane for Cases R2 and R6 at the moment of precipitation.

imply that, increasing the relative humidity will lead to a more asymmetric porous membrane structure with a thinner skin layer. From these profiles, the percentages of dense skin layers were determined as 0.58% and 0.46%, when relative humidity of air is 25% and 50%, respectively. When the mid part of the cross sections of these two membranes shown in Figs. 4 and 11 were analyzed, it was found that with increased relative humidity, porosity in that section increased as predicted by the model. In addition, the pore size decreased as was also observed by Park et al. [49] for membranes prepared by water vapor-induced phase separation.

4.5. Effect of air velocity

The effect of increased air velocity, i.e., forced convection conditions was usually investigated for a combination of dry/wet phase inversion techniques to produce defect free, ultrahigh flux, asymmetric membranes with ultrathin skin layers [50–54]. To investigate the effect of forced convection on the structure of the dry-cast membranes, cellulose acetate solutions cast on a glass plate were allowed to evaporate by blowing air across the membrane surface with a blower. Experimental conditions for this case are denoted as Case R7 and are shown in Table 1. Corresponding composition paths predicted by the model shown in Fig. 12 indicate that neither the air side nor the support side enter the two-phase region. This prediction implies that, when the membrane is dried under strong forced convection conditions, phase separation will not take place and a uniformly dense coating devoid of substantial microstructure will result. This prediction was supported by the scanning electron micrograph of the final film morphology illustrated in Fig. 13. It can be seen that the cross-sectional morphology is dense and non-porous. The optical property of the film, which was translucent, is also consistent with both SEM analysis and model predictions.

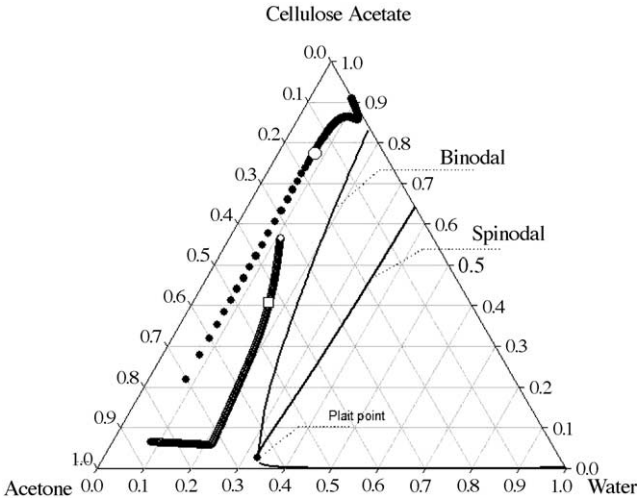

Fig. 12. Concentration paths of water, acetone and cellulose acetate for Case R7: (◯) solution/air interface; (□) solution/substrate interface.

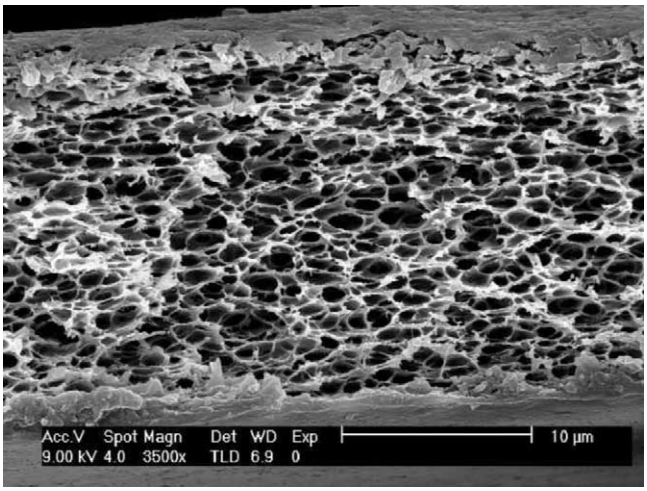

Fig. 11. Scanning electron micrograph of the membrane cast from a ternary water/cellulose acetate/acetone solution for the casting conditions corresponding to Case R6.

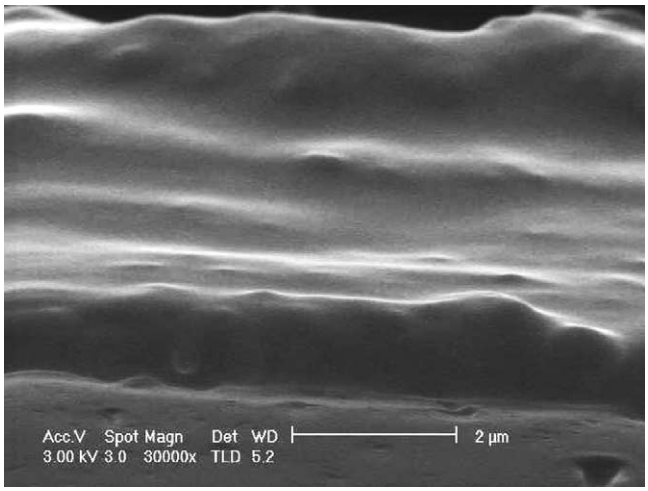

Fig. 13. Scanning electron micrograph of the membrane cast from a ternary water/cellulose acetate/acetone solution for the casting conditions corresponding to Case R7.

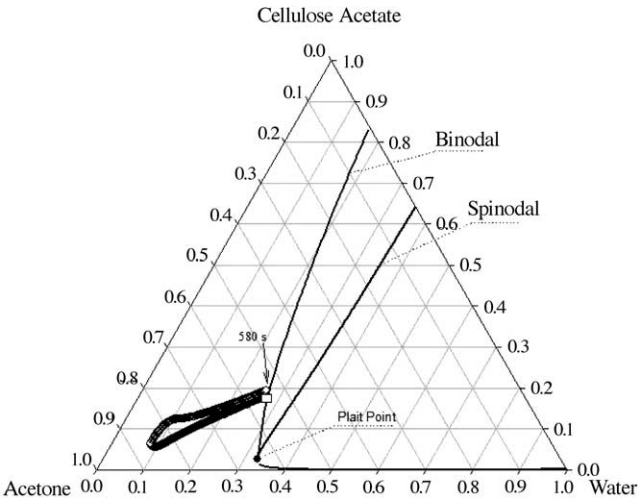

Fig. 14. Concentration paths of water, acetone and cellulose acetate for Case R2: (◯) solution/air interface; (□) solution/substrate interface. Prediction was performed through the insertion of diffusion model using only the principal diffusion coefficients (i.e., the cross diffusion coefficients were set equal to zero).

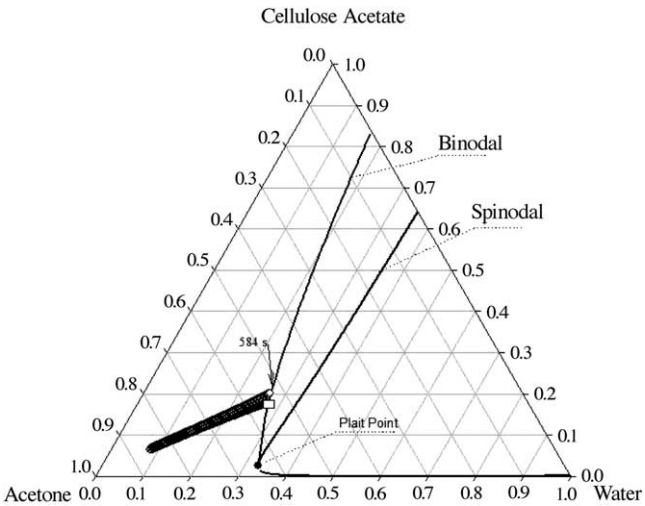

Fig. 15. Concentration paths of water, acetone and cellulose acetate for Case R2: (◯) solution/air interface; (□) solution/substrate interface. Prediction was performed through the insertion of diffusion model in which the cross diffusion coefficients were set equal to zero and the principal diffusion coefficients were estimated by corresponding self-diffusion coefficients.

4.6. *Effect of diffusion formalism*

The predictions of Alsoy Altinkaya and Ozbas [20] have shown that the critical factor for capturing the accurate behavior of membrane formation is the diffusion formalism utilized in the model. Theoretically, diffusion in a ternary system is described by four diffusion coefficients, main diffusion coefficients, D_{11} and D_{22} and cross diffusion coefficients, D_{12} and D_{21}. In all predictions reported so far, the friction-based diffusion model proposed by Alsoy and Duda [29] were utilized. In an attempt to illustrate the importance of accurate diffusion theory on the prediction of the structure of the membrane, simulations corresponding to experimental conditions denoted by Case R2 have been performed for two alternative approximations of ternary diffusion coefficients. Model predictions represented as composition paths on the ternary phase diagrams are shown in Figs. 14 and 15. Concentration paths in Fig. 14 were predicted through the insertion of Alsoy and Duda's diffusion model [29] using only the main diffusion coefficients, i.e., the cross diffusion coefficients D_{12} and D_{21} were set equal to zero. The results in Fig. 15 were obtained using the simplest diffusion theory in which the cross diffusion coefficients are equal to zero and the main diffusion coefficients are predicted by the corresponding self-diffusion coefficients without considering the thermodynamic factor. The predictions shown in Figs. 14 and 15 imply that the final membrane structure will be porous and symmetric since the polymer compositions of two interfaces when they cross the binodal curve, are almost the same. However, the corresponding SEM of the final film morphology shown in Fig. 4 indicate that the membrane structure is highly asymmetric with a thin dense skin layer at the free surface supported by a porous sublayer structure. This structure was accurately predicted by using the full diffusion model as shown previously in Figs. 1 and 2. Misleading conclusions about the structure of the membrane based on the predictions shown in Figs. 14 and 15 clearly point out the need for an accurate formulation of diffusion theory in membrane formation modeling.

5. Conclusions

Scanning electron microscopy has been adapted to investigate the morphology of the membranes and validate the dry-cast model recently developed by us. The composition paths superimposed on the ternary phase diagram and the polymer distribution curves at the first moment of precipitation provided theoretical information about the structure of the membranes such as degree of asymmetry, fraction of dense skin layer, porosity and pore distribution in the sublayer structure. The effects of polymer/nonsolvent ratio in the casting solution, the initial film thickness, evaporation temperature, relative humidity and velocity of air on the ultimate membrane structures were investigated. Results have clearly demonstrated that the final membrane structure is quite sensitive to these preparation conditions. In this work, one of our primary focuses was to illustrate the effect of diffusion formulation on the predictions of the final membrane structures. We have found that accurate formulation of diffusion theory forms the basis of the membrane formation modeling and simplifications in the theory may lead to misleading conclusions about the ultimate structure of the membrane. The comparisons between model predictions and morphological studies were found to be quite good. In addition, the predictive ability of the model was confirmed by gravimetric measurements performed in our earlier work [20]. Consequently, we believe that optimization of the initial dynamics of commercial

membrane casting processes can be advanced with the aid of our model predictions. Obviously, this study presents one of the few techniques toward validating the model. Other experimental results such as permeability measurements and light intensity data can be used to evaluate the model.

References

[1] C. Cohen, G.B. Tanny, S. Prager, Diffusion controlled formation of porous structures in ternary polymer systems, J. Polym. Sci. Polym. Phys. Ed. 17 (1979) 477.

[2] L. Yilmaz, A.J. McHugh, Modeling of asymmetric membrane formation. I. Critique of evaporation models and development of a diffusion equation formalism for the quench period, J. Membr. Sci. 28 (1986) 287.

[3] A.J. Reuvers, C.A. Smolders, Formation of membrane by means of immersion precipitation. Part II. The mechanisms of formation of membranes prepared from the system cellulose acetate–acetone–water, J. Membr. Sci. 34 (1987) 67.

[4] C.S. Tsay, A.J. McHugh, Mass transfer modeling of asymmetric membrane formation by phase inversion, J. Polym. Sci., Part B: Polym. Phys. 28 (1990) 1327.

[5] C.S. Tsay, A.J. McHugh, The combined effects of evaporation and quench steps on asymmetric membrane formation by phase inversion, J. Polym. Sci., Part B: Polym. Phys. 29 (1991) 1261.

[6] C.S. Tsay, A.J. McHugh, Mass transfer dynamics of the evaporation step in membrane formation by phase inversion, J. Membr. Sci. 64 (1991) 81.

[7] C.S. Tsay, A.J. McHugh, A rationale for structure formation during phase inversion, J. Polym. Sci., Part B: Polym. Phys. 29 (1992) 1261.

[8] L.P. Cheng, Y.S. Soh, A.H. Dwan, C.C. Gryte, An improved model for mass transfer during the formation of polymeric membranes by the immersion–precipitation processes, J. Polym. Sci., Part B: Polym. Phys. 32 (1994) 1413.

[9] I.M. Wienk, R.M. Boom, M.A.M. Beerlage, A.M.W. Bulte, C.A. Smolders, H. Strathmann, Recent advances in the formation of phase inversion membranes made from amorphous or semi-crystalline polymers, J. Membr. Sci. 113 (1996) 361.

[10] P. van de Witte, P.J. Dijkstra, J.W.A. van den Berg, J. Feijen, Phase separation processes in polymer solutions in relation to membrane formation, J. Membr. Sci. 117 (1996) 1.

[11] B.F. Barton, A.J. McHugh, Modeling of dynamics of membrane structure formation in quenched polymer solutions, J. Membr. Sci. 166 (2000) 119.

[12] Y.D. Kim, J.Y. Kim, H.K. Lee, S.C. Kim, Anew modeling of asymmetric membrane formation in rapid mass transfer system, J. Membr. Sci. 190 (2001) 69.

[13] S.K. Karode, A. Kumar, Formation of polymeric membranes by immersion precipitation: an improved algorithm for mass transfer calculations, J. Membr. Sci. 187 (2001) 287.

[14] H. Matsuyama, Y. Takida, T. Maki, M. Teramoto, Preparation of porous membrane by combined use of thermally induced phase separation and immersion precipitation, Polymer 43 (2002) 5243.

[15] H. Matsuyama, S. Berghmans, D.R. Lloyd, Formation of anisotropic membranes via thermally induced phase separation, Polymer 40 (1999) 2289.

[16] D.R. Lloyd, K.E. Kinzer, H.S. Tseng, Microporous membrane formation via thermally induced phase-separation. 1. Solid liquid-phase separation, J. Membr. Sci. 52 (1990) 239.

[17] S.S. Shojaie, W.B. Krantz, A.R. Greenberg, Dense polymer film and membrane formation via the dry cast process. Part I. Model development, J. Membr. Sci. 94 (1994) 255.

[18] S.S. Shojaie, W.B. Krantz, A.R. Greenberg, Dense polymer film and membrane formation via the dry cast process. Part II. Model validation and morphological studies, J. Membr. Sci. 94 (1994) 281.

[19] H. Matsuyama, M. Teramoto, T. Uesaka, Membrane formation and structure development by dry cast process, J. Membr. Sci. 135 (1997) 271.

[20] S. Alsoy Altinkaya, B. Ozbas, Modeling of asymmetric membrane formation by dry-casting method, J. Membr. Sci. 230 (2004) 71.

[21] L. Zeman, T. Fraser, Formation of air-cast cellulose acetate membranes. Part I. Study of macrovoid formation, J. Membr. Sci. 84 (1993) 93.

[22] M. Pekny, A. Greenberg, V. Khare, J. Zartman, W.B. Krantz, P. Todd, Macrovoid formation in dry-cast cellulose acetate membranes: buoyancy studies, J. Membr. Sci. 205 (2002) 11.

[23] M. Pekny, J. Zartman, W.B. Krantz, A. Greenberg, P. Todd, Flow-visualization during macrovoid formation in dry-cast cellulose acetate membranes, J. Membr. Sci. 211 (2003) 71.

[24] S. Alsoy, J.L. Duda, Influence of swelling and diffusion-induced convection on polymer sorption processes, AIChE J. 48 (2002) 1849.

[25] B.E. Eichinger, P.J. Flory, Thermodynamics of polymer solutions. 1. Natural rubber and benzene, J. Trans., Faraday Soc. 64 (1968) 2035.

[26] B.E. Eichinger, P.J. Flory, Thermodynamics of polymer solutions. 3. Polyisobutylene and cyclohexane, J. Trans., Faraday Soc. 64 (1968) 2061.

[27] M. Wolf, J.H. Wendorff, Modified equation of state treatment for volume changes of mixing, Polym. Commun. 31 (1990) 226.

[28] K. Sasahara, H. Uedaira, Volume and compressibility changes on mixing aqueous solutions of the amino acid and poly(ethylene glycol), Colloid Polym. Sci. 272 (1994) 385.

[29] S. Alsoy, J.L. Duda, Modeling of multicomponent drying of polymer films, AIChE J. 45 (1999) 896.

[30] S. Alsoy, Modeling of polymer drying and devolatilization processes, Ph.D. thesis, The Pennsylvania State University, University Park, 1998.

[31] J.M. Zielinski, S. Alsoy, Onsager consistency checks for multicomponent diffusion models, J. Polym. Sci., Part B: Polym. Phys. 39 (2001) 1496–1504.

[32] L. Yilmaz, A.J. McHugh, Analysis of nonsolvent–solvent–polymer phase diagrams and their relevance to membrane formation modeling, J. Appl. Polym. Sci. 31 (1986) 997.

[33] B. Ozbas, Modeling of asymmetric membrane formation by dry-casting method, M.Sc. thesis, Izmir Institute of Technology, Izmir, 2001.

[34] J.-M. Cheng, D.-M. Wang, F.-C. Lin, J.-Y. Lai, Formation and gas flux of asymmetric PMMA membranes, J. Membr. Sci. 109 (1996) 93.

[35] J.-Y. Lai, F.-C. Lin, C.-C. Wang, D.-M. Wang, Effect of nonsolvent additives on the porosity and morphology of asymmetric TPX membranes, J. Membr. Sci. 118 (1996) 49.

[36] J.-Y. Lai, F.-C. Lin, C.-C. Wang, D.-M. Wang, Effect of nonsolvent additives on the porosity and morphology of asymmetric TPX membranes, J. Membr. Sci. 118 (1996) 49.

[37] L.-P. Cheng, T.-H. Young, W.-M. You, Formation of crystalline EVAL membranes by controlled mass transfer process in water–DMSO–EVAL copolymer systems, J. Membr. Sci. 145 (1998) 77.

[38] K.W. Broadhead, P.A. Tresco, Effects of fabrication conditions on the structure and function of membranes formed from poly(acrylonitrile–vinylchloride), J. Membr. Sci. 147 (1998) 235.

[39] T.-H. Young, D.-J. Lin, J.-J. Gau, W.-Y. Chuang, L.-P. Cheng, Morphology of crystalline Nylon-610 membranes prepared by the immersion-precipitation process: competition between crystallization and liquid–liquid phase separation, Polymer 40 (1999) 5011.

[40] K.J. Brodbeck, J.R. DesNoyer, A.J. McHugh, Phase inversion dynamics of PLGA solutions related to drug delivery. Part II. The role of solution thermodynamics and bath-side mass transfer, J. Controlled Release 62 (1999) 333.

[41] J. Kurdi, Y. Tremblay, Preparation of defect-free asymmetric membranes for gas separations, J. Appl. Polym. Sci. 73 (1999) 1471.
[42] J. Won, H.C. Park, U.Y. Kim, Y.S. Kang, S.H. Yoo, J.Y. Jho, The effect of dope solution characteristics on the membrane morphology and gas transport properties: PES/-BL/NMP system, J. Membr. Sci. 162 (1999) 247.
[43] J. Won, H.J. Lee, Y.S. Kang, The effect of dope solution characteristics on the membrane morphology and gas transport properties. 2. PES/-BL system, J. Membr. Sci. 176 (2000) 11.
[44] W.-Y. Chuang, T.-H. Young, W.-Y. Chiu, C.-Y. Lin, The effect of polymeric additives on the structure and permeability of poly(vinyl alcohol) asymmetric membranes, Polymer 41 (2000) 5633.
[45] I.-C. Kim, H.-G. Yoon, K.-H. Lee, Formation of integrally skinned asymmetric polyetherimide nanofiltration membranes by phase inversion process, J. Appl. Polym. Sci. 84 (2002) 1300.
[46] S.-C. Fan, Y.-C. Wang, C.-L. Li, K.-R. Lee, D.-J. Liaw, H.-P. Huang, J.-Y. Lai, Effect of coagulation media on membrane formation and vapor permeation performance of novel aromatic polyamide membrane, J. Membr. Sci. 204 (2002) 67.
[47] N.A. Mohamed, A.O.H. Al-Dossary, Structure–property relationships for novel wholly aromatic polyamide-hydrazides containing various proportions of *para*-phenylene and *meta*-phenylene units. III. Preparation and properties of semi-permeable membranes for water desalination by reverse osmosis separation performance, Eur. Polym. J. 39 (2003) 1653.
[48] T.H. Young, J.-H. Huang, W.-Y. Chuang, Effect of evaporation temperature on the formation of particulate membranes from crystalline polymers by dry-cast process, Eur. Polym. J. 38 (2002) 63.
[49] H.C. Park, Y.P. Kim, H.Y. Kim, Y.S. Kang, Membrane formation by water vapor induced phase inversion, J. Membr. Sci. 156 (1999) 169.
[50] I. Pinnau, W. Koros, Structures and gas separation properties of asymmetric polysulfone membranes made by dry, wet, and dry/wet phase inversion, J. Appl. Polym. Sci. 43 (1991) 1491.
[51] I.D. Sharpe, A.F. Ismail, S.J. Shilton, A study of extrusion shear and forced convection residence time in the spinning of polysulfone hollow fiber membranes for gas separation, Sep. Purification Technol. 17 (1999) 101.
[52] A.F. Ismail, B.C. Ng, W.A.W. Abdul Rahman, Effects of shear rate and forced convection residence time on asymmetric polysulfone membranes structure and gas separation performance, Sep. Purification Technol. 33 (2003) 255.
[53] A.F. Ismail, P.Y. Lai, Effects of phase inversion and rheological factors on formation of defect-free and ultrathin-skinned asymmetric polysulfone membranes for gas separation, Sep. Purification Technol. 33 (2003) 127.
[54] I. Ani, A.F. Ismail, M. Noorhayati, S.J. Shilton, Measurement of rheologically induced molecular orientation using attenuated total reflection infrared dichroism in reverse osmosis hollow fiber cellulose acetate membranes and influence on separation performance, J. Membr. Sci. 213 (2003) 45.